Review Article



# The macrosphere model—an embolic stroke model for studying the pathophysiology of focal cerebral ischemia in a translational approach

**Maureen Walberer[1,2,3], Maria Adele Rueger[1,2]**

[1]Department of Neurology, University Hospital of Cologne, Cologne, Germany; [2]Max-Planck-Institute for Metabolism Research, Cologne, Germany; [3]Animal Welfare Office, University of Cologne, Germany

*Correspondence to:* Dr. med. vet. Maureen Walberer, DVM. Animal Welfare Officer, University of Cologne, Cologne, Albertus-Magnus-Platz, 50923 Cologne, Germany. Email: maureen.walberer@uni-koeln.de.

**Abstract:** The main challenge of stroke research is to translate promising experimental findings from the bench to the bedside. Many suggestions have been made how to achieve this goal, identifying the need for appropriate experimental animal models as one key issue. We here discuss the macrosphere model of focal cerebral ischemia in the rat, which closely resembles the pathophysiology of human stroke both in its acute and chronic phase. Key pathophysiological processes such as brain edema, cortical spreading depolarizations (CSD), neuroinflammation, and stem cell-mediated regeneration are observed in this stroke model, following characteristic temporo-spatial patterns. Non-invasive *in vivo* imaging allows studying the macrosphere model from the very onset of ischemia up to late remodeling processes in an intraindividual and longitudinal fashion. Such a design of pre-clinical stroke studies provides the basis for a successful translation into the clinic.

**Keywords:** Macrosphere model; embolic stroke model; translational stroke model; permanent middle cerebral artery occlusion (permanent MCAo)

Submitted Feb 21, 2015. Accepted for publication Feb 24, 2015.
doi: 10.3978/j.issn.2305-5839.2015.04.02
**View this article at:** http://dx.doi.org/10.3978/j.issn.2305-5839.2015.04.02

## Introduction

In the past years, stroke research has encountered one major problem: numerous therapeutic agents that proved quite effective in experimental animal models failed to show any efficacy in human clinical trials. Thus, the recanalization of the occluded vessel within a limited time frame remains the only effective treatment, since—due to negative clinical trials—not one substance out of the plethora of neuroprotective drugs identified in pre-clinical studies has later achieved regulatory approval for this indication. To overcome this problem known as the 'translational road block in stroke research', leading researchers in the field have provided several suggestions (1-4).

One key issue identified to hinder the translation of pre-clinical research into the clinic is the use of experimental stroke models that do not sufficiently resemble the clinical reality of cerebral ischemia (2). Pathophysiological events occurring in the days and weeks after stroke, such as neuroinflammation, cortical spreading depolarizations (CSD), and stem cell-mediated regeneration, need to be taken into account when evaluating the usefulness of an experimental animal model, and should ideally model the human situation (2,5).

Moreover, in a translational approach, preclinical studies should be designed in the same manner as clinical trials, and ideally use the same assays to monitor therapeutic efficacy. Non-invasive *in vivo* imaging using Magnetic-Resonance-Imaging (MRI) and Positron-Emission-Tomography (PET) plays an important role in this regard. Those imaging tools allow monitoring key pathophysiological processes longitudinally and intraindividually over time, such as cerebral blood flow (6), brain edema (7,8), neuroinflammation (9,10), and stem cell-mediated regeneration (11,12).

Along these lines, we here elaborate on the macrosphere model of focal cerebral ischemia, and compare it to other established experimental stroke models.

## Overview over frequently used animal stroke models

For the induction of focal cerebral ischemia in the rats, many different surgical techniques can be used. Basically, endovascular and non-endovascular procedures can be distinguished. In the following, the most frequently used animal stroke models are summarized. *Table 1* gives an overview over the typical characteristics of each model compared to the macrosphere model and to human stroke.

### *Endovascular models*

#### Suture model

The suture model described first in 1986 by Koizumi *et al*. (13) is the most widely used experimental stroke model to study the pathophysiology of focal cerebral ischemia and to evaluate novel therapies. This model can be used to induce both a permanent as well as a transient occlusion of the middle cerebral artery (MCA). Since its first publication, the suture model has been modified by many working groups to optimize its success rates (14-21). To achieve MCA occlusion (MCAo), a nylon filament is inserted through an arteriotomy of the common carotid artery (CCA), anterograde behind the origin of the MCA. Blocking the blood flow to the MCA results in reproducible infarcts within the MCA territory (13-21). If reperfusion is to be achieved, the thread is withdrawn at latest 90 minutes after MCAo (17,18,20). This animal model is easy to use, relatively little invasive, and produces reproducible infarcts.

#### Thromboembolic model

Kudo *et al*. were the first to describe a thromboembolic model for the induction of focal cerebral ischemia (22). In the meanwhile, many variations of this model for optimizing the technique as well as its success rates are reported (23-28). The thromboembolic model closely resembles a common etiology of human stroke, since thrombi are generated and then used for the occlusion of the cerebral artery. Consequently, this model is most suitable for the preclinical evaluation of thrombolytic agents, such as rt-PA (23).

The preparation and structure of thrombi vary widely in the literature. In most cases, autologous (less frequently heterologous) blood is used, which is clotted by the addition of thrombin or other methods. Many authors use clots derived from blood, while others make use of blood components. The prepared thrombi (one single larger or several small ones) are injected in the internal carotid artery (ICA) via an arteriotomy of the CCA, or via a stump created of the external carotid artery (ECA) (22,24).

### *Non-endovascular models*

#### Photothrombosis model

This model was first described by Watson *et al*. in 1985 (29) and makes use of a photosensitive dye to occlude small cortical vessels. First, Rose Bengal solution is injected into the femoral vein, followed by illumination of the cortical surface through the intact skull bone for about 20 minutes, using a fiber optic cold light source with an intensity of 560 nm. This irradiation causes a photochemical reaction of the intravascular Rose Bengal, leading to local thrombosis and vascular occlusion, generating reproducible infarcts that are limited to the cortex (29). Many modifications of this model are reported, e.g., use of laser beams instead of a cold light source (30-34).

#### Direct distal MCAo models

In all these models, a subtemporal craniotomy has to be first performed in order to expose the MCA. Depending on the specific method, the MCA will be occluded directly by a clip (35), a ligation (36-38) or cauterization (37,39) under visual control. In the clip model, a reperfusion of the MCA can be induced by removing the clip (35).

## The macrosphere model of focal cerebral ischemia

### *Surgical method*

The macrosphere model is an endovascular embolic stroke model resembling cardiogenic and arterio-arterial embolism as the main etiology of human stroke. In this model described first by Gerriets *et al*. (40), permanent occlusion of the MCA in rats is induced by $TiO_2$-spheres (*Figure 1A*). Therefore, the macrosphere model mimics arterio-arterial embolism of "hard" atherosclerotic plaque material as the most frequent cause of human stroke (41,42).

In more detail, first a PE-50 tubing is filled with saline, and a defined number of $TiO_2$ "macrospheres" of 0.315 to 0.355 mm in diameter (BRACE® GmbH) are prepared. Depending on the experiment, between one and six macrospheres may be used. After the dissection of extracranial arteries and transection of the ECA, the PE-50 catheter

 

**Table 1** Direct comparison of the findings in human stroke and after MCAo by different stroke models in rats

| Obser-vation | Human ischemic stroke | Macrosphere model | Suture model | Thromboembolic model | Photothrombotic model | Direct distal MCAo models |
|---|---|---|---|---|---|---|
| Cause of vessel occlusion | Cerebral embolism: embolism of blood clots or artherosclerotic plaque material. Atherothrombotic stroke: thrombosis by blood clots, narrowing of blood vessels to the brain caused by atherosclerosis or other particles | Embolization of 1-6 $TiO_2$ spheres mimicking atherosclerotic plaque material | Insertion of a nylon filament | Embolization of synthesized autologous or heterologous blood clots | Local thrombosis by a photochemical reaction (photocoagulation) | Direct occlusion by clip, ligation or cauterization |
| Craniotomy | Used as therapeutic intervention in large stroke | None | None | None | None | Required for these models |
| Reperfusion | Possible and desired | No controlled or uncontrolled reperfusion | Controlled as well as uncontrolled reperfusion possible | Controlled as well as uncontrolled reperfusion possible | None | Controlled reperfusion possible when using clip, no uncontrolled reperfusion |
| Variability of infarct | High variability in infarcts | Infarct size depends on the number of spheres | Reproducible and homogenous infarcts | Interindividual variability of infarct | Reproducible and homogenous infarcts | Reproducible and homogenous infarcts |
| Affected brain regions | Cortical and/or subcortical tissue affected, depending on occluded vessel and collateralization | Cortical and subcortical areas of the MCA territory | Permanent model: cortical and subcortical areas of the MCA territory; Transient model: depending on the duration of occlusion time; only subcortical areas of the MCA territory are involved | Cortical and subcortical areas of the MCA territory | Circumscribed pure cortical lesion | Cortical and subcortical areas of the MCA territory |
| Hyperthermia | Not primarily | None | Yes, if the occlusion lasts for more than 90 minutes | None | None | None |
| Post-ischemic inflammation | Microglia activation starts ≥3 days reaching its maximum within one week after stroke onset. | Microglia activation starts at day 3 reaching its maximum at day 7 after MCAo | Transient model: microglia activation starts at 22 h after MCAo | Not known | Microglia activation starts at day 3 after MCAo | Microglia activation starts 48-72 h after MCAo |
| | Infiltration of macrophages/ microglia in the infarct core at day 7 after MCAo | Infiltration of macrophages/ microglia in the infarct core at day 6-8 after MCAo | Infiltration of macrophages/microglia in the infarct core after 6 hours. Permanent model: not known | | Infiltration of macrophages/ microglia in the infarct core at day 7 after MCAo | Infiltration of macrophages/ microglia in the infarct core at day 3 after MCAo or later |
| Secondary chronic inflammation | In the thalamus of the affected hemisphere from week 4 onwards for at least 12 months | In the thalamus of the affected hemisphere from day 7 onwards for at least 7 months | Not known | Not known | Not known | Not known |

MCA, middle cerebral artery; MCAo, MCA occlusion.

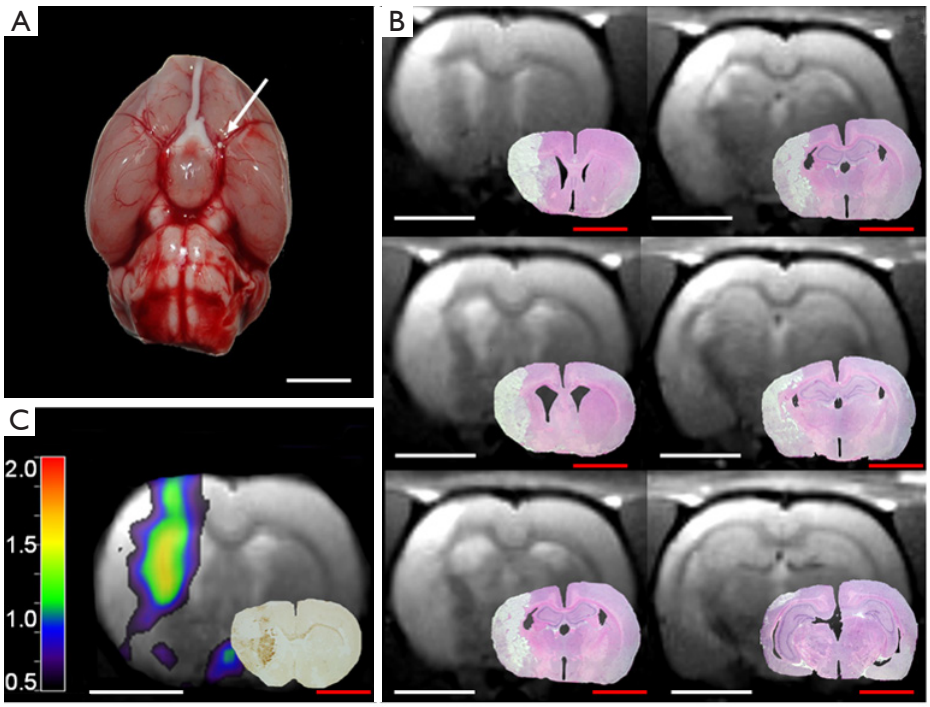


**Figure 1** Exemplary findings 3 weeks after induction of focal cerebral ischemia by the macrosphere model. (A) Basal view of the rat brain displaying the intracerebral arteries following MCAo by macrosphere-injection. One macrosphere (white arrow) is located in the origin of the MCA. (White bar: 5,000 µm). (B) Representative images of T2-weighted MRI from rostral (left column, upper image) to caudal direction delineating the typical ischemic territory 3 weeks after induction of ischemia. (White bar: 5,000 µm). Insets: respective corresponding histological slides stained with hematoxylin and eosin verified the ischemic damage after 3 weeks. (Red bar: 5,000 µm). (C) *In vivo* imaging of neuroinflammation using [$^{11}$C]PK11195-PET fused on T2-weighted MRI at 3 weeks after macrosphere embolization. (Scale: PK-binding potential; white bar: 5,000 µm). Accumulation of [$^{11}$C]PK11195 can be clearly identified within the peri-infarct zone. Inset: in the corresponding immunhistological slide, microglia activation is visualized by staining for MHC class II (right column, lower image). (Red bar: 5,000 µm). MCA, middle cerebral artery; MCAo, MCA occlusion.

is inserted into the stump of the ECA via an arteriotomy, forwarded to the carotid bifurcation, and fixed in place. The macrospheres are injected one-by-one with only a small amount of saline (~0.05 mL), so the spheres move passively into the ICA and are transported by the blood flow through the circle of Willis, blocking the main stem of the MCA. Afterwards, the tubing is removed, and the stump of the ECA is ligated (40).

The failure rates indicating an insufficient occlusion of the MCA by the macrospheres varied dependent on the used numbers of spheres (60-80%) (8,40,43,44).

### *Characteristics of the macrosphere model*

The macrosphere model can be operated as a remote occlusion model, i.e., occlusion of the MCA can be postponed to a defined time point after the actual surgery, and then be achieved from a spatial distance. This specifically allows for the timed occlusion of the vessel while the rat is lying in the MRI-scanner (8,45), the PET-scanner (6), or the Laser-speckle setup (44), and thus for multimodal imaging of the hyperacute phase of stroke (5). In studies utilizing the macrosphere model with remote occlusion, a slight modification of the surgical setup is suggested in order to minimize the risk of a dislocation of the tubing when manipulating the animal (e.g., placement in the restrainer or animal holder) (8). In this modified model, the ECA and the pterygopalatine branch of the ICA are ligated. The filled catheter is inserted through an arteriotomy of the CCA into the ICA until the tip of the

 

tubing is located distal to the origin of the pterygopalatine artery. The macrospheres are then inserted in the ICA by a slow injection of 0.2 mL of saline blocking the blood flow to the MCA (32). Using other experimental stroke models, only few studies performing remote MCAo and monitoring the hyperacute phase of stroke in rodents have been published to date (46-54). In all those studies, remote occlusion of the MCA was performed using the permanent or temporal suture model, making the macrosphere model the first embolic stroke model to allow for remote occlusion. Several modifications for optimizing this technique regarding an improvement of the success rate have been reported (46-54). However, compared to the macrosphere model, remote occlusion in the suture model is technically more difficult, thus requiring more training for the surgeon.

In contrast to various models of permanent MCAo achieved by clipping (36), ligation (36-48) or cauterization (37,39) of the vessel, no craniotomy is required for the macrosphere model. This constitutes a major benefit in preclinical studies, since craniotomy itself has neuroprotective effects (7,55-59), and is performed in large ("malignant") human stroke if the increased intracranial pressure by brain edema cannot be sufficiently reduced by conservative therapeutic strategies (60). Moreover, craniotomy interferes with distinct processes of interest following cerebral ischemia, since it mechanically induces CSD, and elicits neuroinflammation. Furthermore, craniotomy may cause several effects such as subarachnoid hemorrhage, cerebral infection, and cerebrospinal fluid leakage (61), as well as potential injury risk of brain tissue (62). Thus, distal MCAo models with craniotomy represent a non-physiological insult (63), and should be avoided to serve the translational aspect.

The macrosphere model evokes infarcts that are homogenous in extent and localization, and closely resemble human stroke by affecting cortical as well as subcortical areas (*Figure 1B*) (9,40,43). In contrast, the photothrombosis model of stroke affects exclusively the cortex (64). The homogeneity of infarcts produced in the macrosphere model is comparable to the permanent suture model if 4-6 spheres are used, as the origin of the MCA is then completely occluded (9,40,43). If only fewer spheres (1,2) are used, the induced damage is quite heterogeneous, depending on the branches of the vessel that are occluded (10,44). This interindividual variability of infarcts might actually be desired in some context, with the resulting infarct pattern resembling human stroke caused by a partially disintegrated thrombus, such as after a partially successful thrombolysis. This situation could also be mimicked with other (thrombo-)embolic stroke models, but with the risk of an unwanted premature reperfusion at an unknown time-point by spontaneous lysis of the thrombi (65). A similar complication can occur in the suture model due to an insufficient fixation of the thread within the vessel, or due to its physical characteristics (66,67). Other complications of the suture model that can be avoided using the macrosphere model include (I) vessel perforation and subarachnoid/intracerebral hemorrhage caused by too deep insertion of the suture; or (II) failure to induce stroke if the suture is not inserted deep enough (50). In order to reduce the risk of any inappropriate suture insertion to a minimum, Laser-Doppler flowmetry is used frequently, but requires a small craniotomy with the disadvantages discussed above (66). In contrast, the macrospheres will lodge in the same place every time (68).

In the macrosphere model using 6 spheres or less, blood flow to the hypothalamic artery is not blocked, so hypothalamic injury with subsequent hyperthermia is avoided. This represents a stark contrast to the suture model of permanent ischemia (40,43,69-72). Since hyperthermia increases infarct volume, results in clinical deterioration, and influences post-ischemic neuroinflammation, the avoidance of hypothalamic injury is preferred when testing the effects of potential therapeutic agents in preclinical studies (73-77). In a former study, we investigated the neuroprotective effects of the NMDA-antagonist MK-801 in focal cerebral ischemia, when ischemia was induced either by the macrosphere model, or by the permanent suture model. The data showed that neuroprotection occurred only under normothermic conditions using the macrosphere model, while it was not observed in the permanent suture model due to hyperthermia (43).

Due to the nature of the macrospheres, this stroke model cannot be used in a reperfusion paradigm, constituting the main limitation of this model.

### *Cerebral blood flow and metabolism*

In the macrosphere model, the spheres lead to a complete tight and reliable occlusion of the MCA, blocking the entire blood flow within this vessel as revealed by nano-computed tomography (nano-CT) (68). However, due to a certain amount of remaining perfusion via various collateral pathways, parts of the tissue within the MCA territory may still be perfused for a certain time. Within the first 30 minutes after MCAo, the regional cerebral blood flow (rCBF) decreases to 38-65% of baseline rCBF (6).

 

Juenemann *et al*. have shown that the cerebral blood flow of the total ischemic hemisphere is reduced by 82% (78). For the suture model of permanent ischemia, those numbers have been found to be comparable, with a reduction of rCBF by 70-90% in the ischemic hemisphere (66,78). Of note is that this remaining perfusion observed in the suture model is caused not only by collateral pathways but by an inadvertent bypass-perfusion along the filament (68).

We evaluated the early spatio-temporal development of rCBF and metabolism in the macrosphere model using PET and the radiotracers [$^{15}$O]$H_2O$, directly measuring blood flow, and [$^{18}$F]-2-fluoro-2-deoxy-D-glucose (FDG), as surrogate marker for glucose metabolism (6). We observed functionally relevant alterations in rCBF only within the first 30 minutes after macrosphere injection, supporting the development of an ischemic core within the same short time-frame as in other rat models of permanent cerebral ischemia (79-84). Interestingly, [$^{18}$F]FDG-PET with kinetic modelling (net FDG-influx rate constant Ki, FDG-transport rate constant K1) predicted the exact later fate of each voxel of tissue as early as 60 minutes after induction of ischemia (6). This multimodal imaging method allows to distinguish immediately damaged tissue, representing the early infarct core, from the ischemic penumbra, defined by primarily affected but still viable tissue (6). This is of immense interest in the development of novel treatments for stroke, since the ischemic penumbra as the "tissue-at-risk" is still accessible to appropriate therapeutic interventions.

## Brain edema

The remote occlusion technique allows studying the evolving ischemia in the macrosphere model within the MRI-scanner. Using this *in vivo* imaging method, the development of cytotoxic and vasogenic brain edema in the hyperacute phase of stroke were accurately defined (32). The cytotoxic edema measured as apparent diffusion coefficient (ADC) by MRI appears as early as 5 minutes after MCAo, and reaches its final extent after 45 minutes (8), being in accordance with other models of focal and global cerebral ischemia in different animal species (54,85-87). This immediate occurrence of the cytotoxic edema after injection of macrospheres again indicates that this technique provides a prompt and reliable occlusion of the MCA without procedural delay. The formation of the vasogenic edema indicating the breakdown of the blood brain barrier (BBB) is detected as early as 20-35 minutes after MCAo by an increase of T2-relaxation time determined by T2-weighted MRI (8). Imaging data on the disintegration of the BBB in the macrosphere model were confirmed by the measurements of the midline shift on T2-weighted MRI and histologically using Evans Blue extravasation (45). This early BBB breakdown distinguishes the macrosphere model from other stroke models that observe the vasogenic edema only after 90 minutes (88,89).

### *Cortical spreading depolarizations (CSD)*

Lesions to the cortical surface such as an ischemic focus elicit CSD that occur in well-characterized temporo-spatial patterns, and are associated with local changes in blood flow (90-92). In human hemispheric stroke, CSD contribute to lesion progression (93), and therefore constitute a relevant therapeutic target. In the macrosphere model, we investigated the changes in blood flow (rCBF) evoked by the CSD during and after MCAo by Laser Speckle Contrast Imaging (44). Immediately after injection of the macrospheres, there is a fast and gradual drop of rCBF, followed by the propagation of the first CSD concentrically from the border of the ischemic territory outwards into unaffected tissue, crossing almost the whole hemisphere. Multiple, subsequent secondary waves later travel circumferentially around the lesion for several hours (44).

These results are similar to those from CSD induction by direct application of potassium to the cortex of rats and cats (94-96). In a model of direct occlusion of the distal branch of the MCA requiring craniotomy, the CSD waves show a similar circumferential propagation around the ischemic core (97). To our knowledge, in the suture model of stroke, immediate monitoring of CSD propagation has not yet been performed, most likely due to technical difficulties. Later imaging, however, showed similar findings (98,99).

### *Post-ischemic inflammation*

Focal cerebral ischemia elicits characteristic neuroinflammatory responses involving both resident and blood-derived immune cells as well as a cascade of humoral factors. The temporo-spatial characteristics of neuroinflammation have been meticulously described for various animal models of stroke (100-106). Likewise, neuroinflammation occurs after human stroke, and has been characterized using MRI- and PET-imaging (107-112). Neuroinflammation plays an important role in the post-ischemic cascade following cerebral ischemia, having an impact on infarct volume

 

and demarcation as well as on tissue repair und functional outcome (113,114).

Interestingly, in commonly used experimental stroke models, the temporo-spatial patterns of neuroinflammation differ relevantly from those in humans. In human stroke, microglia activation as a surrogate marker of neuroinflammation starts not earlier than 3 days after onset of the infarct, reaching its maximum within one week (108-110). In experimental ischemia involving reperfusion, both microglia activation as well as invasion of blood-borne cells is typically accelerated, starting as early as 22 hours after ischemia (100,115-118). Moreover, the up-regulation of cytokines released by glia cells occurs quite early in commonly used stroke models (119-124). Thus, in order to develop novel treatment strategies for stroke, an experimental stroke model should be chosen to closely resemble the dynamics of post-ischemic inflammation according to the human situation (5). We investigated post-ischemic neuroinflammation after focal cerebral ischemia induced by the macrosphere model based on the key features microglia activation, macrophages infiltration throughout the infarct and phagocytic accumulation (124). Furthermore, we analyzed pro- and anti-inflammatory cytokines (125) as potential biomarkers in human stroke from cerebrospinal fluid or blood (126). Interestingly, macrosphere-induced focal cerebral ischemia very closely resembled the characteristic dynamics of human neuroinflammation, particularly the slow time course in the post-ischemic cascade (125). It is of note that some other models of permanent MCAo including photothrombosis show a similar delayed timeline of post-ischemic neuroinflammation, starting as late as 48-72 hours after induction of infarct (100-106).

In order to initiate clinical studies on the modulation of post-ischemic neuroinflammation, reliable imaging protocols need to be established that allow for both stratifying patients according to inflammation patterns, as well for monitoring the therapeutic efficacy of any treatment strategy. Thus, animal stroke models should allow for *in vivo* imaging (I) with the same imaging modality used in humans to facilitate translation; (II) in a non-invasive fashion to allow longitudinal monitoring in an intraindividual fashion; and (III) in long-term investigations over several months to better mimic the clinical situation.

We investigated neuroinflammation in the macrosphere model using a multimodal imaging protocol including T2-weighted MRI as well as PET with the radiotracers [$^{11}$C]PK11195 and [$^{18}$F]FDG (9). Similar study protocols are performed in human clinical studies (112), allowing the translational evaluation of the macrosphere model. Seven days after stroke onset, kinetic modelling of [$^{18}$F]FDG PET-data defines 3 infarct zones: infarct core (low rCBF and a decreased [$^{18}$F]FDG metabolic rate), infarct margin (reduced rCBF with a regular [$^{18}$F]FDG metabolic rate) and peri-infarct zone (normoperfused tissue with an increased [$^{18}$F]FDG metabolic rate) (9). Restricted to the peri-infarct zone, [$^{11}$C]PK11195 uptake as surrogate parameter for cellular neuroinflammation was observed in all animals independent of the location and size of the ischemic infarct (9). Interestingly, neuroinflammatory processes detected by PET were accompanied by a massively increased energy demand, posing the peri-infarct zone at risk of secondary tissue damage, and suggesting that it should be considered for therapeutic interventions.

In order to fully characterize the whole extent of neuroinflammation in the macrosphere model, we performed long-term investigations of neuroinflammation, repeatedly imaging animals from the acute until the chronic phase of stroke for up to 7-month after embolization of macrospheres (10,115). We observed the maximum of post-ischemic neuroinflammation at day 7—in the border zone of the ischemic core—that disappears around six weeks after MCAo (*Figure 1C*) (10). However, inflammation persists in remote locations such as the thalamus of the affected hemisphere, representing secondary inflammation, for at least 7 months after stroke onset (10). This phenomenon observed in the thalamus using *in vivo* imaging was confirmed histologically, and characterized by activated microglia co-localizing with iron deposits around plaque-like amyloid deposits, as well as with neuronal loss. Similar observations on inflammation-associated neurodegeneration have been made in the late phase of human stroke (126,127). Thus, the macrosphere model mimics even the very late chronic phase of human stroke, while—to our knowledge—similar studies do not yet exist in other stroke models in rats.

The temporo-spatial characteristics of cell-mediated neuroinflammation in the macrosphere model were characterized in even further detail in an immunohistopathological study. Up to 56 days after MCAo, four infarct zones were characterized by their specific patterns of neuroinflammation (infarct core, infarct margin, demarcation zone, peri-infarct zone) (128). Interestingly, infarct demarcation was characterized by the expression and secretion of the proteoglycan NG2 as an active process separating between necrotic and unaffected tissue, suggesting that this process has crucial impact on secondary neurodegeneration after focal cerebral ischemia and should

 

thus be of interest regarding functional outcome (128).

### *Regeneration*

Cerebral ischemia elicits an endogenous regenerative response marked by the proliferation of neural stem cells (NSC) in the brain and their mobilization and migration from their niches towards the ischemic lesion (64,129,130). Enhancing the mobilization of endogenous NSC after stroke by e.g., pharmacological means results in an enhanced functional recovery of experimental animals (131-133). Thus, mobilizing the endogenous NSC niche constitutes a promising future target in stroke therapy. In order to establish such experimental paradigms, non-invasive imaging needs to span the bridge between bench and bedside. Using the macrosphere model of stroke, we established an imaging assay using PET with the radiotracer 3'-deoxy-3'-[$^{18}$F]fluoro-l-thymidine ([$^{18}$F]FLT) to monitor the mobilization of endogenous NSC in the live rat brain (11). This assay has since facilitated the identification of several promising therapeutic agents that increase NSC survival and/or proliferation (12,134-136).

## Conclusions

The macrosphere model of embolic stroke mimics the pathophysiological aspects of human stroke most accurately, both in the acute as well in the chronic phase of stroke. Since this model easily allows for the remote vessel occlusion within the MRI- or PET-scanner, it allows for the non-invasive *in vivo* monitoring of various post-ischemic processes longitudinally over time in individual animals. Thus, the macrosphere model is extremely cwell characterized with regards to the temporo-spatial dynamics of cerebral blood flow, metabolism, neuroinflammation, cortical spreading depressions, and stem cell-mediated regeneration, constituting it an adept model to conduct pre-clinical research in. We propose to consider this stroke model for experimental stroke studies in an intraindividual and longitudinal approach in order to facilitate a successful translation of pre-clinical findings into the clinical situation.

## Acknowledgements

*Funding:* This work was supported by the 'Marga und Walter Boll-Stiftung' (#210-12-12).
*Disclosure:* The authors declare no conflict of interest.

## References

1. Herson PS, Traystman RJ. Animal models of stroke: translational potential at present and in 2050. Future Neurol 2014;9:541-51.
2. Endres M, Engelhardt B, Koistinaho J, et al. Improving outcome after stroke: overcoming the translational roadblock. Cerebrovasc Dis 2008;25:268-78.
3. Dirnagl U, Macleod MR. Stroke research at a road block: the streets from adversity should be paved with meta-analysis and good laboratory practice. Br J Pharmacol 2009;157:1154-6.
4. Dirnagl U, Endres M. Found in translation: preclinical stroke research predicts human pathophysiology, clinical phenotypes, and therapeutic outcomes. Stroke 2014;45:1510-8.
5. Walberer M, Dennin MA, Schroeter M. Comment on: Rodent stroke model guidelines for preclinical stroke trials (1st edition). J Exp Stroke Transl Med 2009;2:49-51.
6. Walberer M, Backes H, Rueger MA, et al. Potential of early [(18)F]-2-fluoro-2-deoxy-D-glucose positron emission tomography for identifying hypoperfusion and predicting fate of tissue in a rat embolic stroke model. Stroke 2012;43:193-8.
7. Gerriets T, Stolz E, Walberer M, et al. Middle cerebral artery occlusion during MR-imaging: investigation of the hyperacute phase of stroke using a new in-bore occlusion model in rats. Brain Res Brain Res Protoc 2004;12:137-43.
8. Walberer M, Ritschel N, Nedelmann M, et al. Aggravation of infarct formation by brain swelling in a large territorial stroke: a target for neuroprotection? J Neurosurg 2008;109:287-93.
9. Schroeter M, Dennin MA, Walberer M, et al. Neuroinflammation extends brain tissue at risk to vital peri-infarct tissue: a double tracer [11C]PK11195- and [18F]FDG-PET study. J Cereb Blood Flow Metab 2009;29:1216-25.
10. Walberer M, Jantzen SU, Backes H, et al. In-vivo detection of inflammation and neurodegeneration in the chronic phase after permanent embolic stroke in rats. Brain Res 2014;1581:80-8.
11. Rueger MA, Backes H, Walberer M, et al. Noninvasive imaging of endogenous neural stem cell mobilization in vivo using positron emission tomography. J Neurosci 2010;30:6454-60.
12. Rueger MA, Muesken S, Walberer M, et al. Effects of minocycline on endogenous neural stem cells after experimental stroke. Neuroscience 2012;215:174-83.

 

13. Koizumi J, Yoshida Y, Nazakawa T, et al. Experimental studies of ischemic brain edema: a new experimental model of cerebral embolism in rats in which re circulation can be introduced in the ischemic area. Jpn J Stroke 1986;8:1-8.
14. Belayev L, Alonso OF, Busto R, et al. Middle cerebral artery occlusion in the rat by intraluminal suture. Neurological and pathological evaluation of an improved model. Stroke 1996;27:1616-22; discussion 1623.
15. Astrup J, Siesjö BK, Symon L. Thresholds in cerebral ischemia - the ischemic penumbra. Stroke 1981;12:723-5.
16. Kuge Y, Minematsu K, Yamaguchi T, et al. Nylon monofilament for intraluminal middle cerebral artery occlusion in rats. Stroke 1995;26:1655-7; discussion 1658.
17. Longa EZ, Weinstein PR, Carlson S, et al. Reversible middle cerebral artery occlusion without craniectomy in rats. Stroke 1989;20:84-91.
18. Matsushima K, Hakim AM. Transient forebrain ischemia protects against subsequent focal cerebral ischemia without changing cerebral perfusion. Stroke 1995;26:1047-52.
19. Nagasawa H, Kogure K. Correlation between cerebral blood flow and histologic changes in a new rat model of middle cerebral artery occlusion. Stroke 1989;20:1037-43.
20. Lourbopoulos A, Karacostas D, Artemis N, et al. Effectiveness of a new modified intraluminal suture for temporary middle cerebral artery occlusion in rats of various weight. J Neurosci Methods 2008;173:225-34.
21. Türeyen K, Vemuganti R, Sailor KA, et al. Ideal suture diameter is critical for consistent middle cerebral artery occlusion in mice. Neurosurgery 2005;56:196-200; discussion 196-200.
22. Kudo M, Aoyama A, Ichimori S, et al. An animal model of cerebral infarction. Homologous blood clot emboli in rats. Stroke 1982;13:505-8.
23. Busch E, Krüger K, Hossmann KA. Improved model of thromboembolic stroke and rt-PA induced reperfusion in the rat. Brain Res 1997;778:16-24.
24. Kaneko D, Nakamura N, Ogawa T. Cerebral infarction in rats using homologous blood emboli: development of a new experimental model. Stroke 1985;16:76-84.
25. Overgaard K, Sereghy T, Boysen G, et al. A rat model of reproducible cerebral infarction using thrombotic blood clot emboli. J Cereb Blood Flow Metab 1992;12:484-90.
26. Zhang Z, Zhang RL, Jiang Q, et al. A new rat model of thrombotic focal cerebral ischemia. J Cereb Blood Flow Metab 1997;17:123-35.
27. Wang CX, Yang T, Shuaib A. An improved version of embolic model of brain ischemic injury in the rat. J Neurosci Methods 2001;109:147-51.
28. Zhang RL, Chopp M, Zhang ZG, et al. A rat model of focal embolic cerebral ischemia. Brain Res 1997;766:83-92.
29. Watson BD, Dietrich WD, Busto R, et al. Induction of reproducible brain infarction by photochemically initiated thrombosis. Ann Neurol 1985;17:497-504.
30. De Ryck M, Van Reempts J, Borgers M, et al. Photochemical stroke model: flunarizine prevents sensorimotor deficits after neocortical infarcts in rats. Stroke 1989;20:1383-90.
31. Gu WG, Brännström T, Jiang W, et al. A photothrombotic ring stroke model in rats with remarkable morphological tissue recovery in the region at risk. Exp Brain Res 1999;125:171-83.
32. Matsuno H, Uematsu T, Umemura K, et al. A simple and reproducible cerebral thrombosis model in rats induced by a photochemical reaction and the effect of a plasminogen-plasminogen activator chimera in this model. J Pharmacol Toxicol Methods 1993;29:165-73.
33. Wester P, Watson BD, Prado R, et al. A photothrombotic "ring" model of rat stroke-in-evolution displaying putative penumbral inversion. Stroke 1995;26:444-50.
34. Yao H, Ibayashi S, Sugimori H, et al. Simplified model of krypton laser-induced thrombotic distal middle cerebral artery occlusion in spontaneously hypertensive rats. Stroke 1996;27:333-6.
35. Buchan AM, Xue D, Slivka A. A new model of temporary focal neocortical ischemia in the rat. Stroke 1992;23:273-9.
36. Robinson RG, Shoemaker WJ, Schlumpf M, et al. Effect of experimental cerebral infarction in rat brain on catecholamines and behaviour. Nature 1975;255:332-4.
37. Bederson JB, Pitts LH, Tsuji M, et al. Rat middle cerebral artery occlusion: evaluation of the model and development of a neurologic examination. Stroke 1986;17:472-6.
38. Tamura A, Graham DI, McCulloch J, et al. Focal cerebral ischaemia in the rat: 1. Description of technique and early neuropathological consequences following middle cerebral artery occlusion. J Cereb Blood Flow Metab 1981;1:53-60.
39. Brint S, Jacewicz M, Kiessling M, et al. Focal brain ischemia in the rat: methods for reproducible neocortical infarction using tandem occlusion of the distal middle cerebral and ipsilateral common carotid arteries. J Cereb Blood Flow Metab 1988;8:474-85.
40. Gerriets T, Li F, Silva MD, et al. The macrosphere model: evaluation of a new stroke model for permanent middle cerebral artery occlusion in rats. J Neurosci Methods 2003;122:201-11.
41. Grau AJ, Weimar C, Buggle F, et al. Risk factors, outcome, and treatment in subtypes of ischemic stroke: the German

 

stroke data bank. Stroke 2001;32:2559-66.
42. Stroke Therapy Academic Industry Roundtable (STAIR). Recommendations for standards regarding preclinical neuroprotective and restorative drug development. Stroke 1999;30:2752-8.
43. Gerriets T, Stolz E, Walberer M, et al. Neuroprotective effects of MK-801 in different rat stroke models for permanent middle cerebral artery occlusion: adverse effects of hypothalamic damage and strategies for its avoidance. Stroke 2003;34:2234-9.
44. Kumagai T, Walberer M, Nakamura H, et al. Distinct spatiotemporal patterns of spreading depolarizations during early infarct evolution: evidence from real-time imaging. J Cereb Blood Flow Metab 2011;31:580-92.
45. Gerriets T, Walberer M, Ritschel N, et al. Edema formation in the hyperacute phase of ischemic stroke. Laboratory investigation. J Neurosurg 2009;111:1036-42.
46. Lythgoe MF, Thomas DL, Calamante F, et al. Acute changes in MRI diffusion, perfusion, T(1), and T(2) in a rat model of oligemia produced by partial occlusion of the middle cerebral artery. Magn Reson Med 2000;44:706-12.
47. Morikawa S, Inubushi T, Ishii H, et al. Effects of blood sugar level on rat transient focal brain ischemia consecutively observed by diffusion-weighted EPI and (1) H echo planar spectroscopic imaging. Magn Reson Med 1999;42:895-902.
48. Huang NC, Yongbi MN, Helpern JA. The influence of preischemic hyperglycemia on acute changes in brain water ADCw following focal ischemia in rats. Brain Res 1998;788:137-43.
49. Röther J, de Crespigny AJ, D'Arceuil H, et al. MR detection of cortical spreading depression immediately after focal ischemia in the rat. J Cereb Blood Flow Metab 1996;16:214-20.
50. Li F, Han S, Tatlisumak T, et al. A new method to improve in-bore middle cerebral artery occlusion in rats: demonstration with diffusion- and perfusion-weighted imaging. Stroke 1998;29:1715-9; discussion 1719-20.
51. Kohno K, Back T, Hoehn-Berlage M, et al. A modified rat model of middle cerebral artery thread occlusion under electrophysiological control for magnetic resonance investigations. Magn Reson Imaging 1995;13:65-71.
52. Roussel SA, van Bruggen N, King MD, et al. Monitoring the initial expansion of focal ischaemic changes by diffusion-weighted MRI using a remote controlled method of occlusion. NMR Biomed 1994;7:21-8.
53. Gyngell ML, Busch E, Schmitz B, et al. Evolution of acute focal cerebral ischaemia in rats observed by localized 1H MRS, diffusion-weighted MRI, and electrophysiological monitoring. NMR Biomed 1995;8:206-14.
54. Harris NG, Zilkha E, Houseman J, et al. The relationship between the apparent diffusion coefficient measured by magnetic resonance imaging, anoxic depolarization, and glutamate efflux during experimental cerebral ischemia. J Cereb Blood Flow Metab 2000;20:28-36.
55. Doerfler A, Engelhorn T, Heiland S, et al. Perfusion- and diffusion-weighted magnetic resonance imaging for monitoring decompressive craniectomy in animals with experimental hemispheric stroke. J Neurosurg 2002;96:933-40.
56. Doerfler A, Schwab S, Hoffmann TT, et al. Combination of decompressive craniectomy and mild hypothermia ameliorates infarction volume after permanent focal ischemia in rats. Stroke 2001;32:2675-81.
57. Engelhorn T, Doerfler A, de Crespigny A, et al. Multilocal magnetic resonance perfusion mapping comparing the cerebral hemodynamic effects of decompressive craniectomy versus reperfusion in experimental acute hemispheric stroke in rats. Neurosci Lett 2003;344:127-31.
58. Engelhorn T, Dörfler A, Egelhof T, et al. Follow-up monitoring with magnetic resonance tomography after decompressive trephining in experimental "malignant" hemispheric infarct. Zentralbl Neurochir 1998;59:157-65.
59. Engelhorn T, Doerfler A, Kastrup A, et al. Decompressive craniectomy, reperfusion, or a combination for early treatment of acute "malignant" cerebral hemispheric stroke in rats? Potential mechanisms studied by MRI. Stroke 1999;30:1456-63.
60. Hofmeijer J, Kappelle LJ, Algra A, et al. Surgical decompression for space-occupying cerebral infarction (the Hemicraniectomy After Middle Cerebral Artery infarction with Life-threatening Edema Trial [HAMLET]): a multicentre, open, randomised trial. Lancet Neurol 2009;8:326-33.
61. Carmichael ST. Rodent models of focal stroke: size, mechanism, and purpose. NeuroRx 2005;2:396-409.
62. Leker RR, Constantini S. Experimental models in focal cerebral ischemia: are we there yet? Acta Neurochir Suppl 2002;83:55-9.
63. Bacigaluppi M, Comi G, Hermann DM. Animal models of ischemic stroke. Part two: modeling cerebral ischemia. Open Neurol J 2010;4:34-8.
64. Zhang RL, Zhang ZG, Chopp M. Ischemic stroke and neurogenesis in the subventricular zone. Neuropharmacology 2008;55:345-52.
65. Hossmann KA. Experimental models for the investigation

 

of brain ischemia. Cardiovasc Res 1998;39:106-20.
66. Schmid-Elsaesser R, Zausinger S, Hungerhuber E, et al. A critical reevaluation of the intraluminal thread model of focal cerebral ischemia: evidence of inadvertent premature reperfusion and subarachnoid hemorrhage in rats by laser-Doppler flowmetry. Stroke 1998;29:2162-70.
67. Liu S, Zhen G, Meloni BP, et al. Rodent stroke model guidelines for preclinical stroke trials (1st edition). J Exp Stroke Transl Med 2009;2:2-27.
68. Langheinrich AC, Yeniguen M, Ostendorf A, et al. Evaluation of the middle cerebral artery occlusion techniques in the rat by in-vitro 3-dimensional micro- and nano computed tomography. BMC Neurol 2010;10:36.
69. Gerriets T, Stolz E, Walberer M, et al. Complications and pitfalls in rat stroke models for middle cerebral artery occlusion: a comparison between the suture and the macrosphere model using magnetic resonance angiography. Stroke 2004;35:2372-7.
70. Li F, Omae T, Fisher M. Spontaneous hyperthermia and its mechanism in the intraluminal suture middle cerebral artery occlusion model of rats. Stroke 1999;30:2464-70; discussion 2470-1.
71. Yamashita K, Busch E, Wiessner C, et al. Thread occlusion but not electrocoagulation of the middle cerebral artery causes hypothalamic damage with subsequent hyperthermia. Neurol Med Chir (Tokyo) 1997;37:723-7; discussion 727-9.
72. He Z, Yamawaki T, Yang S, et al. Experimental model of small deep infarcts involving the hypothalamus in rats: changes in body temperature and postural reflex. Stroke 1999;30:2743-51; discussion 2751.
73. Reglodi D, Somogyvari-Vigh A, Maderdrut JL, et al. Postischemic spontaneous hyperthermia and its effects in middle cerebral artery occlusion in the rat. Exp Neurol 2000;163:399-407.
74. Kim Y, Busto R, Dietrich WD, et al. Delayed postischemic hyperthermia in awake rats worsens the histopathological outcome of transient focal cerebral ischemia. Stroke 1996;27:2274-80; discussion 2281.
75. Hajat C, Hajat S, Sharma P. Effects of poststroke pyrexia on stroke outcome: a meta-analysis of studies in patients. Stroke 2000;31:410-4.
76. Chen H, Chopp M, Welch KM. Effect of mild hyperthermia on the ischemic infarct volume after middle cerebral artery occlusion in the rat. Neurology 1991;41:1133-5.
77. Yanamoto H, Nagata I, Niitsu Y, et al. Prolonged mild hypothermia therapy protects the brain against permanent focal ischemia. Stroke 2001;32:232-9.
78. Juenemann M, Goegel S, Obert M, et al. Flat-panel volumetric computed tomography in cerebral perfusion: evaluation of three rat stroke models. J Neurosci Methods 2013;219:113-23.
79. Paul JS, Luft AR, Yew E, et al. Imaging the development of an ischemic core following photochemically induced cortical infarction in rats using Laser Speckle Contrast Analysis (LASCA). Neuroimage 2006;29:38-45.
80. Dunn AK, Bolay H, Moskowitz MA, et al. Dynamic imaging of cerebral blood flow using laser speckle. J Cereb Blood Flow Metab 2001;21:195-201.
81. Memezawa H, Minamisawa H, Smith ML, et al. Ischemic penumbra in a model of reversible middle cerebral artery occlusion in the rat. Exp Brain Res 1992;89:67-78.
82. Li F, Han SS, Tatlisumak T, et al. Reversal of acute apparent diffusion coefficient abnormalities and delayed neuronal death following transient focal cerebral ischemia in rats. Ann Neurol 1999;46:333-42.
83. Li F, Silva MD, Sotak CH, et al. Temporal evolution of ischemic injury evaluated with diffusion-, perfusion-, and T2-weighted MRI. Neurology 2000;54:689-96.
84. Baron JC. Perfusion thresholds in human cerebral ischemia: historical perspective and therapeutic implications. Cerebrovasc Dis 2001;11:2-8.
85. Dijkhuizen RM, de Graaf RA, Tulleken KA, et al. Changes in the diffusion of water and intracellular metabolites after excitotoxic injury and global ischemia in neonatal rat brain. J Cereb Blood Flow Metab 1999;19:341-9.
86. Moseley ME, Cohen Y, Mintorovitch J, et al. Early detection of regional cerebral ischemia in cats: comparison of diffusion- and T2-weighted MRI and spectroscopy. Magn Reson Med 1990;14:330-46.
87. Pierpaoli C, Alger JR, Righini A, et al. High temporal resolution diffusion MRI of global cerebral ischemia and reperfusion. J Cereb Blood Flow Metab 1996;16:892-905.
88. Hoehn M, Nicolay K, Franke C, et al. Application of magnetic resonance to animal models of cerebral ischemia. J Magn Reson Imaging 2001;14:491-509.
89. Siesjö BK. Pathophysiology and treatment of focal cerebral ischemia. Part I: Pathophysiology. (1992). J Neurosurg 2008;108:616-31.
90. Ohta K, Graf R, Rosner G, et al. Calcium ion transients in peri-infarct depolarizations may deteriorate ion homeostasis and expand infarction in focal cerebral ischemia in cats. Stroke 2001;32:535-43.
91. Umegaki M, Sanada Y, Waerzeggers Y, et al. Peri-infarct depolarizations reveal penumbra-like conditions in

 

striatum. J Neurosci 2005;25:1387-94.
92. Dohmen C, Sakowitz OW, Fabricius M, et al. Spreading depolarizations occur in human ischemic stroke with high incidence. Ann Neurol 2008;63:720-8.
93. Dreier JP. The role of spreading depression, spreading depolarization and spreading ischemia in neurological disease. Nat Med 2011;17:439-47.
94. Farkas E, Pratt R, Sengpiel F, et al. Direct, live imaging of cortical spreading depression and anoxic depolarisation using a fluorescent, voltage-sensitive dye. J Cereb Blood Flow Metab 2008;28:251-62.
95. Smith JM, James MF, Bockhorst KH, et al. Investigation of feline brain anatomy for the detection of cortical spreading depression with magnetic resonance imaging. J Anat 2001;198:537-54.
96. Tomita Y, Tomita M, Schiszler I, et al. Repetitive concentric wave-ring spread of oligemia/hyperemia in the sensorimotor cortex accompanying K(+)-induced spreading depression in rats and cats. Neurosci Lett 2002;322:157-60.
97. Nakamura H, Strong AJ, Dohmen C, et al. Spreading depolarizations cycle around and enlarge focal ischaemic brain lesions. Brain 2010;133:1994-2006.
98. Hartings JA, Rolli ML, Lu XC, et al. Delayed secondary phase of peri-infarct depolarizations after focal cerebral ischemia: relation to infarct growth and neuroprotection. J Neurosci 2003;23:11602-10.
99. Luckl J, Zhou C, Durduran T, et al. Characterization of periinfarct flow transients with laser speckle and Doppler after middle cerebral artery occlusion in the rat. J Neurosci Res 2009;87:1219-29.
100. Lehrmann E, Christensen T, Zimmer J, et al. Microglial and macrophage reactions mark progressive changes and define the penumbra in the rat neocortex and striatum after transient middle cerebral artery occlusion. J Comp Neurol 1997;386:461-76.
101. Garcia JH, Kamijyo Y. Cerebral infarction. Evolution of histopathological changes after occlusion of a middle cerebral artery in primates. J Neuropathol Exp Neurol 1974;33:408-21.
102. Schroeter M, Jander S, Witte OW, et al. Heterogeneity of the microglial response in photochemically induced focal ischemia of the rat cerebral cortex. Neuroscience 1999;89:1367-77.
103. Schroeter M, Schiene K, Kraemer M, et al. Astroglial responses in photochemically induced focal ischemia of the rat cortex. Exp Brain Res 1995;106:1-6.
104. Morioka T, Kalehua AN, Streit WJ. Characterization of microglial reaction after middle cerebral artery occlusion in rat brain. J Comp Neurol 1993;327:123-32.
105. Nowicka D, Rogozinska K, Aleksy M, et al. Spatiotemporal dynamics of astroglial and microglial responses after photothrombotic stroke in the rat brain. Acta Neurobiol Exp (Wars) 2008;68:155-68.
106. Lyons SA, Pastor A, Ohlemeyer C, et al. Distinct physiologic properties of microglia and blood-borne cells in rat brain slices after permanent middle cerebral artery occlusion. J Cereb Blood Flow Metab 2000;20:1537-49.
107. Saleh A, Schroeter M, Ringelstein A, et al. Iron oxide particle-enhanced MRI suggests variability of brain inflammation at early stages after ischemic stroke. Stroke 2007;38:2733-7.
108. Gerhard A, Neumaier B, Elitok E, et al. In vivo imaging of activated microglia using [11C]PK11195 and positron emission tomography in patients after ischemic stroke. Neuroreport 2000;11:2957-60.
109. Gerhard A, Schwarz J, Myers R, et al. Evolution of microglial activation in patients after ischemic stroke: a [11C](R)-PK11195 PET study. Neuroimage 2005;24:591-5.
110. Price CJ, Wang D, Menon DK, et al. Intrinsic activated microglia map to the peri-infarct zone in the subacute phase of ischemic stroke. Stroke 2006;37:1749-53.
111. Saleh A, Schroeter M, Jonkmanns C, et al. In vivo MRI of brain inflammation in human ischaemic stroke. Brain 2004;127:1670-7.
112. Thiel A, Radlinska BA, Paquette C, et al. The temporal dynamics of poststroke neuroinflammation: a longitudinal diffusion tensor imaging-guided PET study with 11C-PK11195 in acute subcortical stroke. J Nucl Med 2010;51:1404-12.
113. Becker KJ. Targeting the central nervous system inflammatory response in ischemic stroke. Curr Opin Neurol 2001;14:349-53.
114. Dirnagl U, Iadecola C, Moskowitz MA. Pathobiology of ischaemic stroke: an integrated view. Trends Neurosci 1999;22:391-7.
115. Ames A 3rd, Wright RL, Kowada M, et al. Cerebral ischemia. II. The no-reflow phenomenon. Am J Pathol 1968;52:437-53.
116. Clark RK, Lee EV, White RF, et al. Reperfusion following focal stroke hastens inflammation and resolution of ischemic injured tissue. Brain Res Bull 1994;35:387-92.
117. Kochanek PM, Hallenbeck JM. Polymorphonuclear leukocytes and monocytes/macrophages in the pathogenesis of cerebral ischemia and stroke. Stroke 1992;23:1367-79.
118. Barone FC, Schmidt DB, Hillegass LM, et al. Reperfusion

 

increases neutrophils and leukotriene B4 receptor binding in rat focal ischemia. Stroke 1992;23:1337-47; discussion 1347-8.
119. Buttini M, Sauter A, Boddeke HW. Induction of interleukin-1 beta mRNA after focal cerebral ischaemia in the rat. Brain Res Mol Brain Res 1994;23:126-34.
120. Liu T, Clark RK, McDonnell PC, et al. Tumor necrosis factor-alpha expression in ischemic neurons. Stroke 1994;25:1481-8.
121. Liu T, McDonnell PC, Young PR, et al. Interleukin-1 beta mRNA expression in ischemic rat cortex. Stroke 1993;24:1746-50; discussion 1750-1.
122. Minami M, Kuraishi Y, Yabuuchi K, et al. Induction of interleukin-1 beta mRNA in rat brain after transient forebrain ischemia. J Neurochem 1992;58:390-2.
123. Schroeter M, Küry P, Jander S. Inflammatory gene expression in focal cortical brain ischemia: differences between rats and mice. Brain Res Mol Brain Res 2003;117:1-7.
124. Stoll G, Jander S, Schroeter M. Inflammation and glial responses in ischemic brain lesions. Prog Neurobiol 1998;56:149-71.
125. Walberer M, Rueger MA, Simard ML, et al. Dynamics of neuroinflammation in the macrosphere model of arterio-arterial embolic focal ischemia: an approximation to human stroke patterns. Exp Transl Stroke Med 2010;2:22.
126. Ogawa T, Yoshida Y, Okudera T, et al. Secondary thalamic degeneration after cerebral infarction in the middle cerebral artery distribution: evaluation with MR imaging. Radiology 1997;204:255-62.
127. Pappata S, Levasseur M, Gunn RN, et al. Thalamic microglial activation in ischemic stroke detected in vivo by PET and [11C]PK1195. Neurology 2000;55:1052-4.
128. Claus HL, Walberer M, Simard ML, et al. NG2 and NG2-positive cells delineate focal cerebral infarct demarcation in rats. Neuropathology 2013;33:30-8.
129. Jin K, Minami M, Lan JQ, et al. Neurogenesis in dentate subgranular zone and rostral subventricular zone after focal cerebral ischemia in the rat. Proc Natl Acad Sci U S A 2001;98:4710-5.
130. Arvidsson A, Collin T, Kirik D, et al. Neuronal replacement from endogenous precursors in the adult brain after stroke. Nat Med 2002;8:963-70.
131. Nakatomi H, Kuriu T, Okabe S, et al. Regeneration of hippocampal pyramidal neurons after ischemic brain injury by recruitment of endogenous neural progenitors. Cell 2002;110:429-41.
132. Leker RR, Soldner F, Velasco I, et al. Long-lasting regeneration after ischemia in the cerebral cortex. Stroke 2007;38:153-61.
133. Androutsellis-Theotokis A, Leker RR, Soldner F, et al. Notch signalling regulates stem cell numbers in vitro and in vivo. Nature 2006;442:823-6.
134. Klein R, Blaschke S, Neumaier B, et al. The synthetic NCAM mimetic peptide FGL mobilizes neural stem cells in vitro and in vivo. Stem Cell Rev 2014;10:539-47.
135. Hucklenbroich J, Klein R, Neumaier B, et al. Aromatic-turmerone induces neural stem cell proliferation in vitro and in vivo. Stem Cell Res Ther 2014;5:100.
136. Rueger MA, Schroeter M. In vivo imaging of endogenous neural stem cells in the adult brain. World J Stem Cells 2015;7:75-83.

**Cite this article as:** Walberer M, Rueger MA. The macrosphere model—an embolic stroke model for studying the pathophysiology of focal cerebral ischemia in a translational approach. Ann Transl Med 2015;3(9):123. doi: 10.3978/j.issn.2305-5839.2015.04.02

 